molecular pharmaceutics

Article

pubs.acs.org/molecularpharmaceutics

Filamentous, Mixed Micelles of Triblock Copolymers Enhance Tumor Localization of Indocyanine Green in a Murine Xenograft Model

Tae Hee Kim,[†,‡] Christopher W. Mount,[†] Benjamin W. Dulken,[†] Jenelyn Ramos,[§] Caroline J. Fu,[§] Htet A. Khant,[§] Wah Chiu,[§] Wayne R. Gombotz,[∥] and Suzie H. Pun*[,†]

[†]Department of Bioengineering, University of Washington, 3720 15th Avenue NE, Seattle, Washington 98195, United States

[§]National Center for Macromolecular Imaging, Verna and Marrs McLean Department of Biochemistry and Molecular Biology, Baylor College of Medicine, Houston, Texas 77030, United States

[∥]Omeros Corporation, Seattle, Washington 98101, United States

Supporting Information

ABSTRACT: Polymeric micelles formed by the self-assembly of amphiphilic block copolymers can be used to encapsulate hydrophobic drugs for tumor-delivery applications. Filamentous carriers with high aspect ratios offer potential advantages over spherical carriers, including prolonged circulation times. In this work, mixed micelles composed of poly(ethylene oxide)-poly[(*R*)-3-hydroxybutyrate]-poly(ethylene oxide) (PEO-PHB-PEO) and Pluronic F-127 (PF-127) were used to encapsulate a near-infrared fluorophore. The micelle formulations were assessed for tumor accumulation after tail vein injection to xenograft tumor-bearing mice by noninvasive optical imaging. The mixed micelle formulation that facilitated the highest tumor accumulation was shown by cryo-electron microscopy to be filamentous in structure compared to spherical structures of pure PF-127 micelles. In addition, increased dye loading efficiency and dye stability were attained in this mixed micelle formulation compared to pure PEO-PHB-PEO micelles. Therefore, the optimized PEO-PHB-PEO/PF-127 mixed micelle formulation offers advantages for cancer delivery over micelles formed from the individual copolymer components.

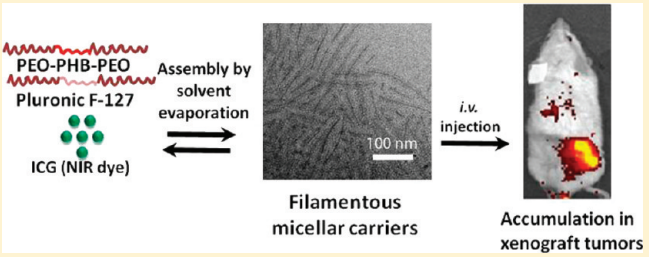

KEYWORDS: *filamentous micelles, indocyanine green, tumor delivery, triblock copolymers*

INTRODUCTION

Chemotherapy remains one of the major treatment approaches for cancer. Though effective, several drawbacks limit the action of these drugs. Most chemotherapeutics are hydrophobic and thus poorly water-soluble. In addition, cancer chemotherapies are generally active against dividing cells, and therefore also affect healthy dividing cells such as those in the bone marrow or digestive tract. This offsite toxicity can be dose-limiting, thereby affecting treatment efficacy. Tumors also frequently develop drug resistances that reduce their responsiveness to certain chemotherapeutics.[1]

Polymeric micelles, self-assembled structures often formed from amphiphilic block copolymers, are promising carriers for chemotherapeutics because they help to address the aforementioned issues.[2,3] In aqueous solutions, the hydrophobic blocks form cores that can serve as reservoirs for hydrophobic molecules while the surrounding hydrophilic block ensures water solubility and stability. Micelle formulations that remain relatively stable *in vivo* enable improved biodistribution, and tumor targeting of encapsulated drugs through the enhanced permeability and retention (EPR) effect.[4] Micelle stability at physiologic conditions is therefore an important property for tumor delivery applications.

Micelle morphology and size depend on specific composition and formulation conditions.[5] Spherical micelles, typically 10–100 nm in size, have been primarily used in drug delivery applications, although several recent studies have reported advantages of filamentous morphologies; for instance, higher drug loading can be obtained with filamentous micelles.[6,7] In addition, Discher and colleagues showed that long filamentous micelles are much less susceptible to phagocytic clearance compared to shorter micelles, resulting in prolonged *in vivo* circulation times (up to one week in mice).[8]

We recently reported a Pluronic F-127 (PF-127, block copolymer of poly(ethylene oxide) and poly(propylene oxide) with composition PEO_{100}-PPO_{65}-PEO_{100}) polymeric micelle that facilitates tumor accumulation of a near-infrared (NIR) dye, indocyanine green (ICG), in xenograft mouse models following intravenous injection.[9] However, two challenges of working with this thermosensitive material are low drug loading efficiency and the need to formulate micelles at elevated temperatures. In parallel studies, we demonstrated that a

Received: August 3, 2011
Revised: November 3, 2011
Accepted: November 27, 2011
Published: November 28, 2011

copolymer composed of poly(ethylene oxide) and poly(3-hydroxybutyrate), hereafter PEO-PHB-PEO, offers high drug loading and stable micellar structures at room temperature.[10] We hypothesized that a mixed micelle formulation of these two triblock copolymers would result in a delivery vehicle that provides efficient drug loading and stability at room and body temperatures, enabling more robust micelle preparations while enhancing distribution of the delivered molecule to tumor sites. The more crystalline PHB block is proposed to offer stability at room temperature while the PF-127 component, due to its thermosensitive nature, provides improved stability at body temperature, the ability to increase drug delivery to multidrug resistant tumors, and the potential for active targeting due to facile chemical conjugation.[8]

Previous studies have demonstrated that mixing two miscible block copolymers in solution generally results in the formation of mixed micelles rather than coexistence of two separate micelle species.[11−13] Mixed micelles have been used successfully to provide improved functionality to micellar formulations for drug delivery applications, and a mixed micelle system, composed of Pluronics L61 and F127, is currently in clinical trials.[14−16] For example, Bae and co-workers have reported mixed micelles composed of a pH-sensitive copolymer that facilitates drug release in acidic tumor environments with a stabilizing copolymer, PEG-PLA (poly(ethylene glycol)-*co*-poly(lactide)).[17−19] The Hsiue group has also reported several formulations of either pH-sensitive or temperature-sensitive copolymers mixed with PEG-PLA copolymers to utilize both the stabilizing effect of the PEG or the ability to conjugate targeting ligands to PEG.[20−22]

In this work, mixed micelle formulations were prepared using various ratios of PEO-PHB-PEO and the thermosensitive PF-127. Confirmation of micelles containing two species of block copolymers was confirmed by fluorescence resonance energy transfer (FRET) studies. The stabilities of the micelle formulations were assessed by encapsulation of ICG, which was used as an indicator for both *in vitro* stability and *in vivo* tumor accumulation. Tumor accumulation was monitored by noninvasive NIR fluorescence imaging using a tumor-bearing mouse model. A mixed micelle formulation with filamentous morphology was identified that exhibited improved passive tumor accumulation when compared with both types of pure micelles.

MATERIALS AND METHODS

Materials. Natural source poly[(*R*)-3-hydroxybutyrate] (PHB), anhydrous diethylene glycol dimethyl ether (diglyme), anhydrous ethylene glycol, dibutyltin dilaurate, 4-(dimethylamino)pyridine (DMAP), triethylamine, and anhydrous dichloromethane were purchased from Sigma Aldrich (St. Louis, MO). Methoxy-poly(ethylene glycol)-monocarboxylic acid (mPEG-COOH, M_w 4900) and fluorenylmethyloxycarbonyl-PEG-monocarboxylic acid (Fmoc-PEG-COOH, M_w 4200) were obtained from Laysan Bio (Arab, AL). Pluronic F-127 (PEO_{100}-PPO_{65}-PEO_{100}, M_w = 12,600) and indocyanine green (ICG) were purchased from Sigma-Aldrich (St. Louis, MO, USA). Tetrabutylammonium iodide (TBAI) and 1,3-*N*,*N*′-dicyclohexylcarbodiimide (DCC) were purchased from Acros Organics (Morris Plains, NJ) and MP Biomedicals (Solon, OH) respectively. Solvents used were ACS grade and obtained from J. T. Baker Chemical Co. (Phillipsburg, NJ) with the exception of chloroform (EMD, Gibbstown, NJ).

Synthesis of PEO-PHB-PEO Triblock Copolymers. PEO-PHB-PEO copolymers were synthesized as previously described.[10,17,23,24] In brief, PHB diol (M_w 2300) was prepared from purified natural high molecular weight PHB by transesterification with diethylene glycol using dibutyltin dilaurate as a catalyst in diglyme. Carboxy-terminated PEO was then conjugated to the PHB diol termini through DCC coupling chemistry. Following fractional precipitation from a mixed solvent of chloroform/diethyl ether, the triblock copolymer was purified by filtration through Amicon regenerated cellulose membranes (MWCO 30 kDa, Millipore, Billerica, MA). Purity was subsequently confirmed by NMR and GPC analysis. The M_w of the triblock as determined by GPC was 16,600 and the M_n was 13,800.

Synthesis of Fmoc-PEO-PHB-PEO Triblock Copolymers. PEO-PHB-PEO triblock with a terminal fluorenylmethyloxycarbonyl (Fmoc) functional group was synthesized by a two-step variation of the previously described triblock synthesis. Briefly, in the first step, PHB-diol and mPEG-COOH were reacted in a 1:1.2 molar ratio with DCC coupling in the presence of DMAP for 48 h to yield PEO-PHB diblock. After filtration of precipitated dicyclohexylurea, the diblock was precipitated in diethyl ether and was characterized by NMR and GPC analysis. PEO-PHB diblock was then reacted at a 1:1.2 ratio with Fmoc-PHB-COOH with DCC coupling in the presence of DMAP to yield an Fmoc-terminated triblock. After filtration of precipitated dicyclohexylurea, the triblock was handled, filtered, and characterized as described above. To expose the reactive amine of the Fmoc functional group, Fmoc-PEO-PHB-PEO was mixed for 1 h at 100 mg/mL in 20% piperidine in DMF (v/v). Liberated Fmoc was detected under UV illumination after isolation via thin-layer chromatography and subsequent iodine staining.

FRET Dye Conjugation and Energy Exchange Measurement. A 488/555 FRET dye pairing was employed to verify the proximity of the two triblock types in solution. An Alexa Fluor 488 succinimidyl ester dye (Molecular Probes) was conjugated to deprotected Fmoc-PEO-PHB-PEO triblock, and Alexa Fluor 555 succinimidyl ester dye was conjugated to the terminal amine of Pluronic F127 triblock after amination using *N*-hydroxysuccinimide and ethylene diamine. Briefly, conjugation was carried out at a 1:1 dye/primary amine ratio in 1× phosphate buffered saline (pH 8) at a polymer concentration of 0.5 mg/mL. The reaction solution was mixed for 20 h, and free dye was removed by multiple filtrations through a MW 3000 molecular weight cutoff centrifuge filter (Pall-Life Sciences). Energy exchange was measured by mixing 10 mg/mL solutions of each polymer at varying ratios and exciting the FRET pair at 488 and 555 nm, recording emission intensity at 565 nm using a Safire 2 microplate fluorimeter (Tecan, Austria).

Preparation of ICG-Encapsulating Mixed Micelles. A solvent evaporation method was implemented to encapsulate ICG within micelles after complexing ICG with TBAI to form a hydrophobic ICG-tetrabutylamine salt, as previously described.[25] Initially, a 1 mM ICG solution was prepared in chloroform with a 6-fold molar excess of TBAI. After 30 min of sonication, the ICG solution was then added dropwise to stirring micelle solutions containing various ratios of PHB triblock (PEO-PHB-PEO) to Pluronic F127 triblock (PEO-PPO-PEO) (10:0, 7:3, 5:5, 3:7, 0:10). The chloroform was evaporated off to incorporate ICG into the hydrophobic cores of mixed micelles. Free ICG was removed using Amicon regenerated cellulose centrifuge filters (MWCO 10000,

Millipore, Billerica, MA), and the remaining ICG-loaded micelle solution was rinsed two times using deionized (DI) water. Purified micelles were resuspended in the original volume of DI water and lyophilized using a Labconco FreeZone 2.5 benchtop freeze-dryer (Labconco, Kansas City, MO).

ICG Loading Efficiency and ICG Content. Lyophilized micelles were weighed and dissolved in 1 mL of dimethyl sulfoxide (DMSO), causing complete dissolution of the micelle and release of the encapsulated ICG. Empty micelles dissolved in DMSO were used as a blank for ICG-loaded micelle samples. The ICG concentration was determined by comparing absorbance at 775 nm to a standard curve of ICG with a squared correlation coefficient of 0.999 in the linear range of 0−12.5 μM in DMSO. ICG content was expressed as the weight ratio between loaded ICG and total weight of ICG-loaded micelle and loading efficiency as the weight percent of encapsulated ICG to total ICG initially used for encapsulation. All loading measurements were performed in triplicate.

CMC Determination. The critical micelle concentration (CMC) of the micelles was determined by measuring the light scattering of serial aqueous dilutions of unloaded micelles using a Wyatt miniDAWN TREOS detector. The peak signal obtained from each sample was plotted against a logarithmic scale of micelle concentration, and the CMC was calculated as the point of intersection between the least-squared regression fits to the baseline detector voltage and the linear region of signal increase.

Measurement of Micelle Sizes. The effective diameters of the mixed micelles (10:0, 7:3, 5:5, 3:7, 0:10 [PHB:PF-127]) prepared at 1 mg/mL was measured using a ZetaPlus dynamic light scattering (DLS) instrument (Brookhaven Instrument Co., Holtsville, NY) at a wavelength of 659 nm with a 90° detection angle at both 25 and 37 °C. Each sample was analyzed in triplicate, and the effective diameter and polydispersity of the micelle formulation were reported.

Micelle Imaging. Select micelle formulations were imaged by cryo-TEM. Micelles were prepared at 37 °C as described above and suspended across a thin layer of vitreous ice by rapid plunging into liquid ethane using Gatan's CP3 Cryo-plunger (Gatan, Pleasanton, CA).[26] Low dose cryo-EM imaging was performed on a JEM 2100 electron microscope (JEOL, Tokyo Japan) operating at 200 kV with a Gatan 626 liquid nitrogen specimen cryo-holder. Images were recorded by Gatan US4000 4k × 4k CCD camera at 21,000−67,000× magnifications.

Aqueous and Thermal Stability Studies. Stability of ICG in mixed micelles was evaluated by measuring decay of fluorescence emission in solution over a period of approximately 10 days. After preparing ICG-encapsulating mixed micelle solutions as described above, samples were dissolved at 10 mg/mL in deionized water and maintained at room temperature or 37 °C in the dark and under slight agitation for the duration of the study. At predetermined intervals, each mixture was sampled and the fluorescence intensity of the sample was evaluated with excitation at 775 nm and emission from 786 to 850 nm.

Cell Lines and Cell Culture. MDA-MB-435 human melanoma cells were cultured in improved MEM (Mediatech Inc., Manassas, VA) with 10% FBS and 1% antibiotic/antimicrobial at 37 °C in 5% CO_2.

Animals and Tumor Implantation. Pathogen free Balb/c mice were housed in separate cages with normal access to food and water and kept on a 12 h light−dark cycle. All experimental procedures were performed in accordance with the protocols approved by the Institutional Animal Care and Use Committee at the University of Washington. To generate tumors, the flanks of 6-week-old male Balb/c mice were shaved and 100 μL of single cell suspension containing 2×10^6 MDA-MB-435 cells in serum-free IMEM was injected subcutaneously under anesthesia.

Tumor Localization Study. ICG and ICG-loaded micelle solutions (150 μL) were injected intravenously (iv) through the tail vein of MDA-MB-435 tumor-bearing mice at a dose of 10 μg of ICG. A second injection was performed with the same dose of ICG and ICG-loaded micelles 30 min following the initial injection. Blood was collected at various time points, and all the mice were sacrificed at the last time point to collect the liver, lung, heart, kidney, spleen, and tumor. A fluorescence-based assay was used to analyze ICG in the biological samples as previously described.[9] Briefly, the blood samples were diluted by adding 100 μL of DMSO to dissociate micelles and analyzed after 10 min. Tissue samples were homogenized with 1 mL of DMSO, followed by overnight extraction at room temperature in the dark. The mixtures of blood and tissues were then centrifuged at 10,000 rpm for 10 min, and the supernatant containing the extracted ICG was measured by fluorescence spectroscopy. The fluorescence intensity of ICG in plasma was normalized by protein content as measured by BCA Protein Assay Kit (Pierce, Rockford, IL). The amount of ICG in tissue was calculated according to a standard curve with a squared correlation coefficient of 0.993 in the linear range of 0−0.25 μg/mL and normalized by weight of tissue. The tissue and plasma samples from the nontreated animals were analyzed to determine the background fluorescence.

RESULTS

Micelle Formulation and Characterization. ICG-encapsulated micelles were prepared by solvent evaporation using PEO-PHB-PEO, PF-127, or mixtures of these two polymers. Particle sizing of the ICG-loaded micelles clearly illustrated temperature-dependent behavior in the micelle architectures (Figure 1A). At room temperature, PEO-PHB-PEO and mixed micelles had average effective diameter ca. 100 nm. No data is available for pure PF-127 because stable micelles are not formed at the evaluated concentration at room temperature. At 37 °C PF-127 micelles formed small, uniform structures with effective diameters of ca. 26 nm while PEO-PHB-PEO micelles were larger with effective diameters of ca. 120 nm. The average hydrodynamic diameter of mixed micelles decreased with increasing PF-127 content. The polydispersity of each formulation at 37 °C is shown in Figure 1B. Polydispersity of pure PF-127 micelles is low (PD = 0.08) while polydispersity of formulations containing PEO-PHB-PEO ranged from PD = 0.26 to 0.28.

DLS assumes spherical particles in its analysis, but the differences in polydispersity indicated the possibility of nonspherical morphologies. Therefore, pure PEO-PHB-PEO micelles, pure PF-127 micelles and 7:3 PEO-PHB-PEO:PF-127 micelles encapsulating ICG were imaged by cryo-TEM. Because temperature-sensitivity was observed with these micelles, micelles were prepared at 37 °C and then flash frozen for analysis. All formulations were prepared in duplicate from two separate solutions and imaged. The observed structures were reproducible between the replicates, and representative images are shown in Figure 2. Filamentous structures were observed for PEO-PHB-PEO and 7:3 PEO-PHB-PEO:PF-127 micelles, with average diameters of 5.40 ± 0.88 nm (n = 49)

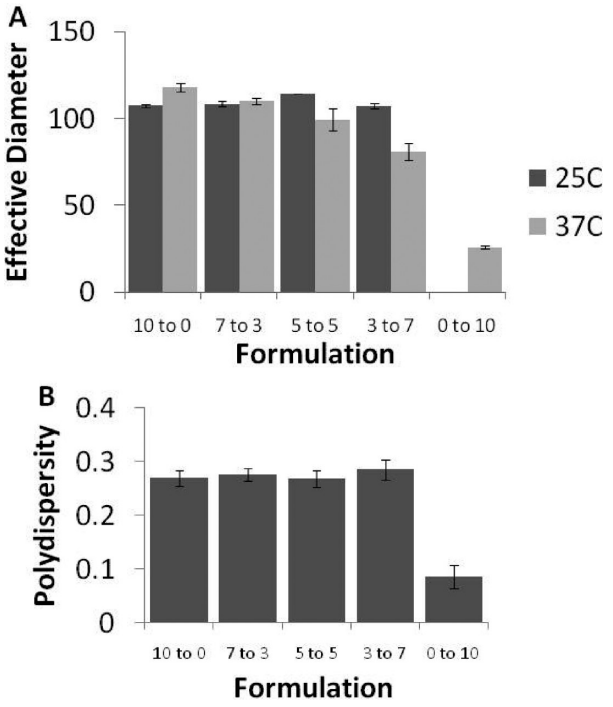

Figure 1. (A) Particle size analysis of ICG-loaded mixed micelles in PBS as a function of micelle composition (PEO-PHB-PEO to PF-127 ratio). Increasing the fraction of PF-127 at 37 °C decreases micelle effective diameter. Stable micelles are not formed with pure PF-127 at room temperature (ND = not determined). (B) Polydispersity of ICG-loaded micelles in PBS at 37 °C.

and 5.25 ± 0.73 nm (n = 48), respectively, while pure PF-127 micelles were spherical in structure with average diameter of 10.00 ± 1.28 nm (n = 54).

To evaluate whether the micelles being formed were in fact mixtures of the two triblock copolymers and not separate populations of each type, FRET studies were conducted. Close spatial proximity of donor-conjugated PEO-PHB-PEO and acceptor-conjugated PF-127 is expected to result in efficient FRET whereas separate populations of PEO-PHB-PEO and PF-127 micelles would not be concentrated enough to result in energy transfer. As shown in Figure 3, energy transfer from donor PEO-PHB-PEO to acceptor PF-127 is observed in all

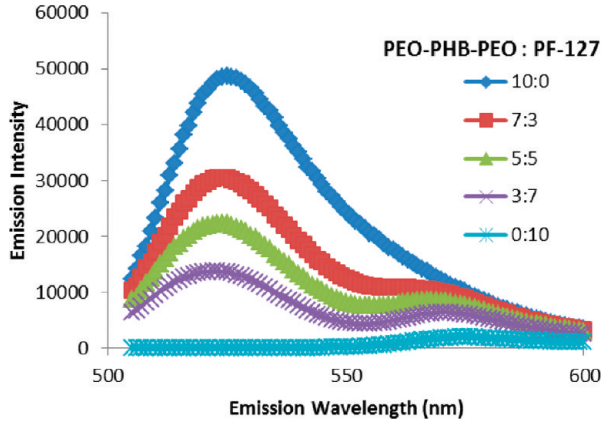

Figure 3. FRET behavior in mixed micelle formulations upon excitation of donor fluorophore. Donor fluorophore (Alexa Fluor 488, peak emission at 519 nm) was conjugated to PEO-PHB-PEO, and acceptor fluorophore (Alexa Fluor 555, peak emission at 565 nm) was conjugated to PF-127. Increasing fraction of PF-127 correlates with decreased ratio of donor/acceptor fluorescence when excited at donor wavelength (488 nm), indicating colocalization of donor/acceptor fluorophores.

mixed micelle formulations, thus confirming that the polymers colocalized in mixed micelle structures.

The effect of mixed micelle polymer ratios on micelle stability was assessed by determining the CMC for each formulation using static light scattering (Supplementary Figure 1 in the Supporting Information).[27] The CMC can be identified as the point at which the refractive index curve deviates significantly from a baseline of 0; a sharp increase in refractive index is indicative of spontaneous macromolecular assembly.[27] The enhancement of stability of the mixed micelles at room temperature by incorporating PEO-PHB-PEO is clearly evident, as micelles with increasing fractional proportions of PEO-PHB-PEO exhibit lower CMC values (Table 1).

ICG Loading and Fluorescence Stability in Micelles. ICG has advantageous fluorescence properties for NIR imaging *in vivo*, but limitations include the molecule's photo, aqueous, and thermal instability.[28,29] Aqueous degradation of the compound occurs as a result of double bond saturation in the molecule's conjugated chain so sequestering the molecule from the solvent radicals that activate this process reduces the rate of its degradation.[29,30] To test the ability of the mixed

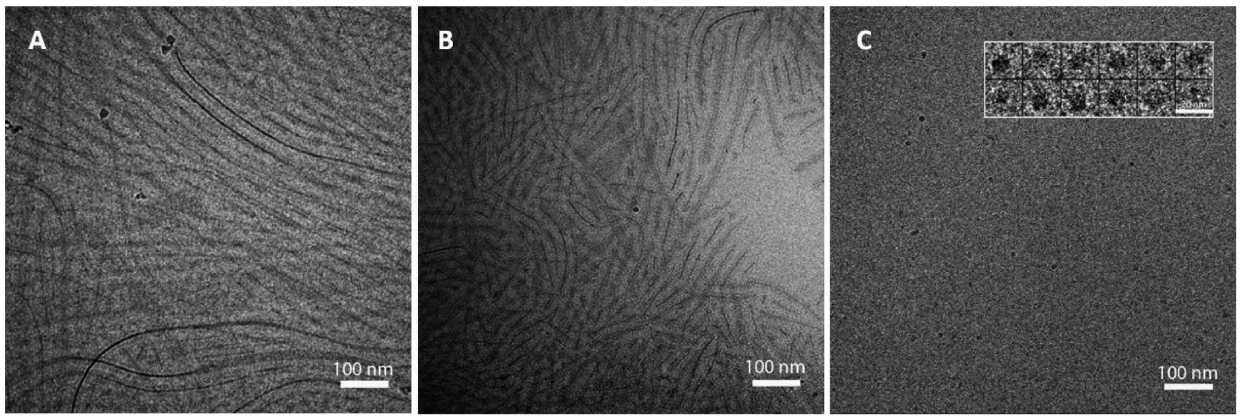

Figure 2. Cryo-EM images of (A) PEO-PHB-PEO micelles, (B) 7:3 PEO-PHB-PEO:PF-127 micelles and (C) PF-127 micelles. Micelles were equilibrated at 37 °C before flash-freezing in liquid ethane. Scale bar in inset of panel C is 20 nm.

Table 1. Critical Micelle Concentrations as Measured by Static Light Scattering and ICG Loading Efficiency for Various Mixed Micelle Formulation Ratios at 25 °C in mg/mL

micelle formulation (PEO-PHB-PEO:PF-127)	CMC (mg/mL)	ICG loading efficiency (%)
10 to 0	0.0135	66.9
7 to 3	0.019	77.9
5 to 5	0.027	80.2
3 to 7	0.042	91.3

micelle systems to stabilize ICG, ICG was loaded into micelles by solvent evaporation. The ICG loading efficiency in the various formulations is shown in Table 1. Loading efficiency in the mixed micelle formulations increases with higher PF-127 content. The ICG loading content ranged from 1 μg of ICG/mg of polymer (10 to 0 formulation) to 1.6 of μg ICG/mg of polymer (3 to 7 formulation). The fluorescence of encapsulated dye was monitored over time at both room temperature and 37 °C (Figure 4). All measurements were normalized to the initial

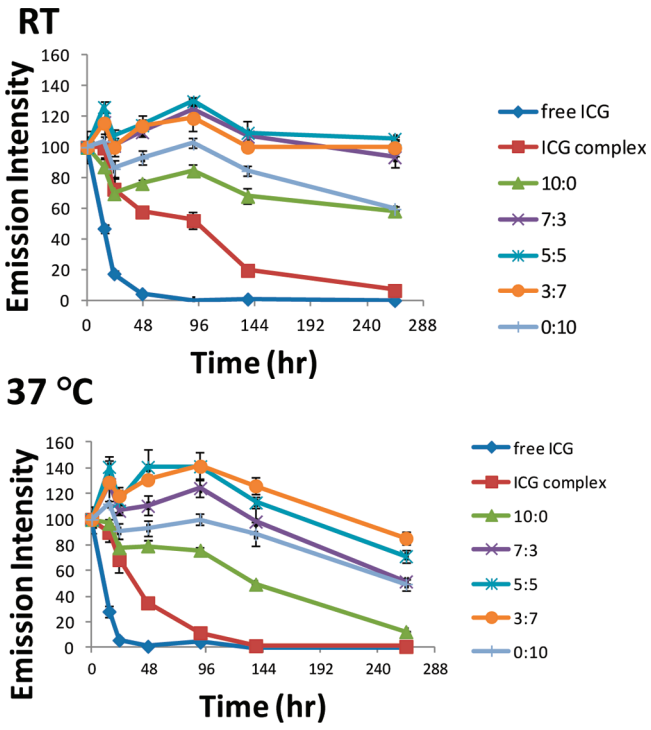

Figure 4. Fluorescence of ICG, ICG-TBA salt, and ICG-micelles maintained in water at room temperature and 37 °C. All measurements are normalized to initial fluorescence emission of respective formulations at t = 0. Samples were excited at 775 nm and emission was read at 815 nm. Triplicate samples were measured for each formulation.

fluorescence at t = 0. At both room temperature and 37 °C, free ICG rapidly degrades to less than 10% of its original fluorescence value within 48 h. All mixed micelle formulations improved ICG stability compared to PEO-PHB-PEO and PF-127 micelles maintaining near 100% of original fluorescence after 10 days at room temperature and above 60% of original fluorescence after 10 days at 37 °C. ICG in PEO-PHB-PEO (10:0) micelles showed significant fluorescence loss at 37 °C compared to room temperature. This decline in ICG fluorescence in PEO-PHB-PEO micelles at 37 °C was mitigated by inclusion of PF-127 in mixed micelle formulations.

Evaluation of ICG-Micelle Formulations *in Vivo*. Free ICG or ICG-micelles were administered to mice by tail vein injection in two sequential injections of 10 μg of ICG per dose per mouse with 30 min between the two injections. We previously showed that double micelle injection results in higher plasma concentrations, perhaps due to saturation of phagocytic cells after the first injection.[9] Blood samples were taken at various time points to compare the relative bioavailability of injected ICG formulations (Figure 5). The

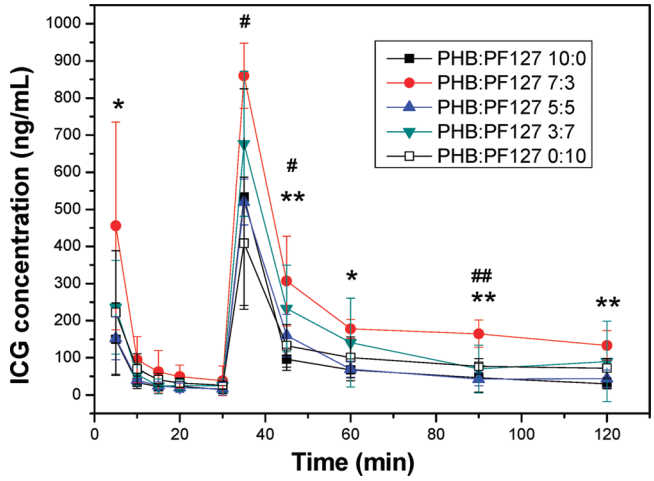

Figure 5. Plot of plasma concentration of ICG vs time for various micelle formulations after intravenous administration. * and ** indicate a statistically significant difference between PEO-PHB-PEO:PF-127 7:3 and PEO-PHB-PEO:PF-127 10:0 using Student's t test, $p < 0.05$ and $p < 0.01$, respectively, n = 5 . # and ## indicate a statistically significant difference between PEO-PHB-PEO:PF-127 7:3 and PEO-PHB-PEO:PF-127 0:10 using Student's t test, $p < 0.05$ and $p < 0.01$, respectively, n = 5.

PEO-PHB-PEO:PF-127 7:3 ICG micelle showed the highest plasma concentrations after both the first and second injections. Area under the curve (AUC) for this formulation was 2.5-fold higher than the 10:0 formulation (p-value = 0.035 in two-sided t test). Interestingly, the AUC for PEO-PHB-PEO:PF-127 3:7 micelles was also higher compared to the pure PEO-PHB-PEO micelles although there is little improvement change in the 5:5 formulation.

To determine efficiency of tumor accumulation, whole-body NIR fluorescence images of ICG were collected 2 and 24 h after administration of ICG to xenograft tumor-bearing mice. At 2 h the fluorescence image is dominated by signal from the liver. However, at 24 h, ICG is mostly eliminated from the body and tumor accumulation is evident (Figure 6). Low levels of fluorescence were observed in spleen, heart, lung and kidney by 24 h postinjection (Supplementary Figure 1 in the Supporting Information), although liver fluorescence is still evident and ~10-fold higher than all organs (data not shown). A comparison of tumor accumulation of the various ICG formulations reveals a trend similar to that observed in the blood circulation data: a polymer ratio of 7:3 results in maximal ICG fluorescence in the vicinity of the tumor (right flank). Moreover, a ratio of 5:5 provides little stabilization of fluorescence intensity when compared to the other groups.

dx.doi.org/10.1021/mp200381c | *Mol. Pharmaceutics* 2012, 9, 135–143

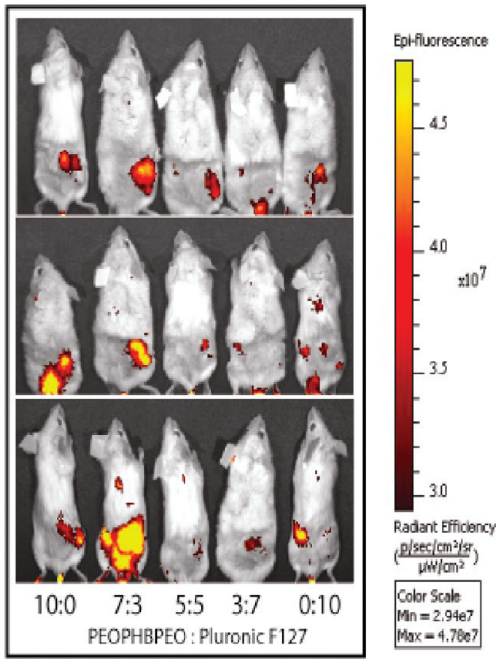

Figure 6. Full body images of mice injected with ICG-micelles 24 h after initial ICG administration. Images acquired using Xenogen Spectrum imager, with excitation at 775 nm and emission at 820 nm. All images are scaled to the same minimum and maximum color values, $n = 3$.

This data was quantified using ROI analysis after excising the tumor tissues.

Tumor tissues that were collected at 24 h are displayed for fluorescence intensity (yellow hot) and size comparison (Figure 7A). Tumor size was not uncharacteristically disperse across groups, and the strongest average signal intensity was also observed in the 7:3 formulation. Region of interest (ROI) analysis to calculate the average radiant efficiency of each tumor was conducted on the tumor tissues collected at 24 h post injection for quantification of ICG fluorescence. Mice treated with the 7:3 mixed micelle formulation showed statistically significant increase in ICG fluorescence signal in the tumor tissue when compared to mice treated with the 10:0 formulation or free ICG (Figure 7B).

DISCUSSION

In this work, mixed micelles of PF-127 and PEO-PHB-PEO (PEO_{5k}-$PHB_{2.3k}$-PEO_{5k}) triblock copolymers were formulated, characterized, and assessed for tumor delivery. ICG was loaded in the micelles as a tool for monitoring micelle stability and *in vivo* biodistribution. PF-127 does not form micelles at room temperature but self-assembles at higher temperatures, thus generating more stable architectures at physiological temperatures.[31] PEO-PHB-PEO contains the highly crystalline PHB hydrophobic block that drives micelle assembly at room temperature. The molecular weights of the two copolymers (~12000 Da) and the block lengths were selected to be similar in order to facilitate micelle formation.

Analysis of the average hydrodynamic radius of the micelles by DLS revealed thermosensitive behavior for the mixed micelles; at 37 °C micelle diameter decreases as PF-127 content increases (Figure 1A). Pure PF-127 micelles had average hydrodynamic diameters of 20 nm, the same size reported previously by Attwood and co-workers for PF-127 micelles in the 35−45 °C range.[32] Lo et al. also recently reported the ability to regulate particle size at elevated temperatures by incorporation of thermosensitive copolymers in mixed micelle constructs.[21] The polydispersities of PEO-PHB-PEO and mixed micelle formulations were higher than the polydispersity of PF-127 micelles, indicating possible nonspherical morphologies (Figure 1B).

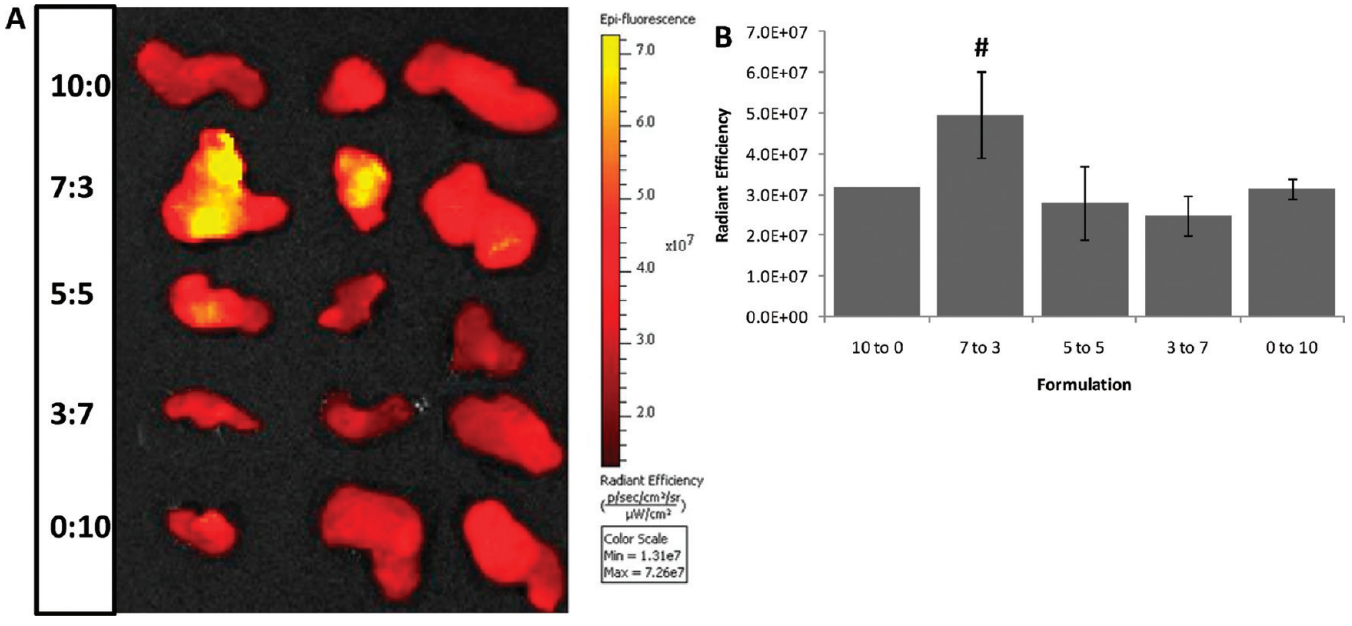

Figure 7. Excised tumor tissues following sacrifice of mice injected with ICG-encapsulating mixed micelles at various PEO-PHB-PEO to PF-127 ratios. (A) Fluorescence image of excised tumor tissues obtained 24 h after initial injection of ICG. (B) Quantification of ICG fluorescence in tumor tissue excised 24 h after injection using ROI analysis. # indicates a statistically significant difference between the 7:3 mixed micelles and 10:0 micelles (one-tailed $p = 0.035$, $n = 3$).

dx.doi.org/10.1021/mp200381c | *Mol. Pharmaceutics* 2012, 9, 135−143

PEO-PHB-PEO, PF-127 and 7:3 PEO-PHB-PEO:PF-127 mixed micelles were therefore imaged by cryo-electron microscopy. PF-127 micelles were uniform and spherical in shape whereas filamentous structures were observed for both PEO-PHB-PEO and 7:3 PEO-PHB-PEO:PF-127 mixed micelles (Figure 2). The filamentous structures were unexpected because the hydrophilic mass fraction ($f_{hydrophilic}$) of these block copolymers is ~80% for PEO-PHB-PEO and ~70% for PF-127. In this regime, most micelles form spherical structures because this morphology is favored when hydrophilic blocks are longer than hydrophobic blocks due to larger available surface area.[33,34]

The filamentous structures observed by cryo-TEM were also quite distinct from wormlike micelles with flexible morphology reported for systems formed from materials such as mPEG-PCL.[6,35] The relatively rigid morphology observed here likely reflects the crystalline nature of the hydrophobic core due to the isotactic PHB. Crystalline phases have been shown to form from PHB-PEO-PHB triblocks but only with isotactic PHB blocks; polymers synthesized from atactic PHB are amorphous.[36] Li et al. analyzed the crystallization behavior of a similar PEO-PHB-PEO triblock copolymer (PEO_{5k}-$PHB_{3.8k}$-PEO_{5k}) by differential scanning calorimetry and found the melting temperatures (T_m) of the PEO and PHB blocks to be 54.1 and 140.2 °C, respectively.[23] Rigid cylindrical structures were also reported by Zhang and co-workers for their crystalline mPEG-poly(caprolactone-*b*-L-lactide) block copolymers (T_m of the hydrophobic block ~150 °C) as compared to the analogous amorphous mPEG-poly(caprolactone-*b*-D,L-lactide) materials, which formed spherical structures.[37]

It should be noted that Li et al. showed by TEM that PEO_{5k}-$PHB_{3.8k}$-PEO_{5k} triblocks formed spherical structures with diameters ~3−70 nm in aqueous solutions instead of the filamentous structures reported here.[38] This difference is likely due to differences in micelle formulation. Li et al. prepared micelles by direct dissolution in water, whereas in order to load hydrophobic drugs into the micelles reported here, micelles were dissolved in a chloroform/water mixture with subsequent evaporation of chloroform. Ravenelle reported that slow evaporation of chloroform (over 2 weeks) from PEO_{5k}-PHB_{1k} diblock copolymers resulted in spherical morphologies with diameters ~50−100 nm whereas rapid evaporation of chloroform over 24 h, similar to the methodology employed here, resulted in rigid filamentous structures.[39]

To confirm that both copolymers were self-assembling in heterogeneous structures rather than segregated micelle populations, each copolymer was labeled with a fluorophore to probe spatial colocalization by means of fluorescent resonance energy transfer (Figure 3). PEO-PHB-PEO was labeled with the donor dye (AlexaFluor 488), while PF-127 was labeled with the acceptor (AlexaFluor 555). When excited at 491 nm, minimal fluorescence emission was detected from the 0:10 (pure PF-127) micelles, indicating that the vast majority of acceptor fluorescence occurred due to resonant energy transfer from excited donor molecules in the molecule's immediate vicinity (30−60 Å).[40] In the mixed micelle formulations, acceptor fluorescence at 565 nm was between 4- and 10-fold higher than in the 0:10 formulations, with the ratio of (donor fluorescence)/(acceptor fluorescence) decreasing with higher fractions of PF-127. These observations provide confirmation that heterogeneous mixed micelles were achieved with this mixture of triblock copolymers.

The CMC of the mixed micelles were measured to assess whether incorporating the PEO-PHB-PEO copolymer would result in stable micelle formation at 25 °C. As anticipated, increasing the fraction of PEO-PHB-PEO significantly decreased the CMC, indicating improved particle stability at room temperature (Table 1). The determined values for each formulation with >50% PEO-PHB-PEO content are similar to the reported value for a similar PEO-PHB-PEO copolymer (0.013 mg/mL for PEO_{5k}-$PHB_{3.8k}$-PEO_{5k}), indicating substantial contribution of the more PHB crystalline core in micelle formulation at room temperature.[23] Several methods were attempted for measuring CMC at 37 °C without success. Typical fluorescence methods such as pyrene or PRODAN encapsulation resulted in low dye incorporation without the chloroform emulsion step, likely due to the crystalline nature of the PHB block.

High content of PEO-PHB-PEO in the micelle formulations resulted in reduced dye loading efficiency, likely due to the higher crystallinity in the cores of these formulations. The ability of polymeric micelles to protect ICG from the aqueous environment significantly reduces the rate of the molecule's degradation and thus stabilizes the molecule's fluorescence.[9,25] At room temperature (Figure 4A), each of the micelle formulations significantly reduces the degradation kinetics of ICG, as monitored by fluorescence measurements, compared to free (unencapsulated) ICG. The mixed micelle formulations provide the best stabilization of the dye. While the ability of polymeric nanocarriers to stabilize the fluorescence of organic dyes is well-known, this mixed micelle system offers the ability to optimize particle formulation for the best stabilization of ICG fluorescence at physiological temperature (Figure 4B).[25,41] The degradation half-life of aqueous ICG is decreased by 30% with an increase in incubation temperature from 22 to 42 °C.[42] At 37 °C, the advantages of micellar encapsulation with the thermosensitive PF-127 copolymer are pronounced, as the 3:7 formulation offers the best stabilization of ICG fluorescence over the time period studied. Because ICG degradation is due to solvent radicals and ions, encapsulation of ICG within a more crystalline core may offer better protection against these agents.

The ICG-loaded micelles were evaluated *in vivo* for plasma clearance kinetics and tumor accumulation by intravenous delivery to a murine xenograft tumor model. Effective passive tumor delivery of nanoparticulate vehicles requires increased circulation half-life for sufficient tumor accumulation to occur via the EPR effect.[43−45] The 7:3 PEO-PHB-PEO:PF-127 mixed micelles provided 2.5-fold higher bioavailability of ICG compared to the pure micelle formulations over the 120 min period of analysis. The CMC of the mixed micelle formulations is lower than that of PF-127 micelles at room temperature (Table 1), and this suggests that the CMC of the mixed micelle formulations may also be lower than PEO-PHB-PEO micelles at 37 °C due to the thermosensitive aggregation behavior of PF-127. The prolonged circulation of the 7:3 PEO-PHB-PEO:PF-127 mixed micelles (Figure 5) may also be attributed to their filamentous shape. Champion and Mitragotri demonstrated using elongated polystyrene worms with high aspect ratios (>20) that negligible phagocytosis was observed compared to spherical morphologies.[46,47] Because the primary clearance mechanism for systemically injected nanoparticles is clearance by the reticuloendothelial system, reduced macrophage uptake is expected to lead to prolonged circulation times. Christian et al. report that flexible poly(ethylene oxide)-*b*-

poly(ε-caprolactone) (PEO-PCL) filamentous micelles remain in murine circulation even 24 h after initial administration due to diffuse fluorescence observed in the mouse.[48] This diffuse fluorescence was not observed in our studies; further increases of *in vivo* stability might be achieved by lengthening the hydrophobic block length of the triblock copolymers to decrease CMC.

Tumor accumulation of the various ICG-micelle formulations was monitored by noninvasive NIR imaging at 24 h postadministration, and the relative tumor fluorescence levels achieved by ICG-micelle formulations correlated well with circulation times (Figure 6). In these images, the brightest signal emanated from the tumors of mice treated with the 7:3 PEO-PHB-PEO:PF-127 mixed micelle formulations. Tumors were then harvested from the mice and directly imaged (Figure 7A). After normalizing the fluorescence intensity signal from each tumor to its area, tumors from mice treated with the 7:3 PEO-PHB-PEO:PF-127 formulation were confirmed to exhibit the highest ICG fluorescence signal (Figure 7B). We previously reported tumor imaging using spherical PF-127 micelles encapsulating ICG. By optimizing a mixed micelle formulation, a 60% increase in tumor-associated fluorescence was achieved.

CONCLUSION

We report mixed micelles encapsulating the NIR fluorophore ICG that were formed from PEO-PHB-PEO and PF-127 block copolymers. The formation of heterogeneous micelles composed of both copolymers was confirmed by FRET analysis. Filamentous morphologies that are relatively rigid compared to filamentous structures formed from polycaprolactone-containing copolymers were observed for the 7:3 mixed micelle formulation likely due to the highly crystalline PHB block. Mixed micelle formulations enhanced the stability of ICG in solution, and the 7:3 PEO-PHB-PEO:PF-127 formulation showed increased circulation times and improved tumor accumulation in a murine xenograft model compared to the other formulations. Advantages of the mixed micelle formulations over pure PEO-PHB-PEO or PF-127 micelles include facile formulation at room temperature, filamentous structures, reduced plasma clearance rate, and increased passive tumor targeting. These formulations are therefore promising for tumor-targeted imaging and drug delivery.

ASSOCIATED CONTENT

Supporting Information

Figure depicting representative ICG fluorescence from major organs and tumor 24 h postinjection of ICG-micelles. This material is available free of charge via the Internet at http://pubs.acs.org.

AUTHOR INFORMATION

Corresponding Author

*University of Washington, Department of Bioengineering, Box 355061, 3720 15th Avenue NE, Seattle, Washington 98195. Phone: (206) 685 3488. Fax: (206) 616 3928. E-mail: spun@u.washington.edu.

Present Address

‡Technical Textile Technology Center, Korea Institute of Industrial Technology (KITECH), Ansan 426-910, Korea.

ACKNOWLEDGMENTS

This work was supported by the funds from the Washington Technology Center, Omeros Corporation and NIH grants (P41RR002250 and RC2GM092599 to W.C.). C.W.M. gratefully acknowledges the Levinson's Emerging Scholars program and Goldwater Foundation for scholarship support. B.W.D. thanks Amgen Scholars program for scholarship support. Xenogen Spectrum imaging was conducted through the Center for Intracellular Delivery of Biologics, funded by Washington State Life Sciences Discovery Fund Grant 2496490. We are grateful to Professors Dennis Discher (University of Pennsylvania) and Timothy Lodge (University of Minnesota) for helpful discussions and advice.

REFERENCES

(1) Krishna, R.; Mayer, L. D. Multidrug resistance (MDR) in cancer—Mechanisms, reversal using modulators of MDR and the role of MDR modulators in influencing the pharmacokinetics of anticancer drugs. *Eur. J. Pharm. Sci.* **2000**, *11* (4), 265−283.

(2) Jones, M. C.; Leroux, J. C. Polymeric micelles—a new generation of colloidal drug carriers. *Eur. J. Pharm. Biopharm.* **1999**, *48* (2), 101−111.

(3) Kataoka, K.; Harada, A.; Nagasaki, Y. Block copolymer micelles for drug delivery: design, characterization and biological significance. *Adv. Drug Delivery Rev.* **2001**, *47* (1), 113−131.

(4) Mikhail, A. S.; Allen, C. Block copolymer micelles for delivery of cancer therapy: Transport at the whole body, tissue and cellular levels. *J. Controlled Release* **2009**, *138* (3), 214−223.

(5) Gaucher, G.; et al. Block copolymer micelles: preparation, characterization and application in drug delivery. *J. Controlled Release* **2005**, *109* (1−3), 169−188.

(6) Cai, S. S.; et al. Micelles of different morphologies—Advantages of worm-like filomicelles of PEO-PCL in paclitaxel delivery. *Pharm. Res.* **2007**, *24* (11), 2099−2109.

(7) Crothers, M.; et al. Solubilisation in aqueous micellar solutions of block copoly(oxyalkylene)s. *Int. J. Pharm.* **2005**, *293* (1−2), 91−100.

(8) Geng, Y.; et al. Shape effects of filaments versus spherical particles in flow and drug delivery. *Nat. Nanotechnol.* **2007**, *2* (4), 249−255.

(9) Kim, T. H.; et al. Evaluation of Temperature-Sensitive, Indocyanine Green-Encapsulating Micelles for Noninvasive Near-Infrared Tumor Imaging. *Pharm. Res.* **2010**, *27* (9), 1900−1913.

(10) Kim, T. H.; et al. The delivery of doxorubicin to 3-D multicellular spheroids and tumors in a murine xenograft model using tumor-penetrating triblock polymeric micelles. *Biomaterials* **2010**, *31* (28), 7386−7397.

(11) Gao, Z. S.; Eisenberg, A. A model of micellization for block-copolymers in solutions. *Macromolecules* **1993**, *26* (26), 7353−7360.

(12) Liu, T. B.; Nace, V. M.; Chu, B. Self-assembly of mixed amphiphilic triblock copolymers in aqueous solution. *Langmuir* **1999**, *15* (9), 3109−3117.

(13) Shim, D. F. K.; Marques, C.; Cates, M. E. Diblock copolymers—comicellization and coadsorption. *Macromolecules* **1991**, *24* (19), 5309−5314.

(14) Alakhov, V.; et al. Block copolymer-based formulation of doxorubicin. From cell screen to clinical trials. *Colloids Surf., B* **1999**, *16* (1−4), 113−134.

(15) Mu, C. F.; et al. The effects of mixed MPEG-PLA/Pluronic (R) copolymer micelles on the bioavailability and multidrug resistance of docetaxel. *Biomaterials* **2010**, *31* (8), 2371−2379.

(16) O'Neil, C. P.; et al. Extracellular matrix binding mixed micelles for drug delivery applications. *J. Controlled Release* **2009**, *137* (2), 146−151.

(17) Kim, D.; et al. Doxorubicin Loaded pH-sensitive Micelle: Antitumoral Efficacy against Ovarian A2780/DOXR Tumor. *Pharm. Res.* **2008**, *25* (9), 2074−2082.

(18) Lee, E. S.; Na, K.; Bae, Y. H. Polymeric micelle for tumor pH and folate-mediated targeting. *J. Controlled Release* **2003**, *91* (1−2), 103−113.
(19) Yin, H. Q.; Bae, Y. H. Physicochemical aspects of doxorubicin-loaded pH-sensitive polymeric micelle formulations from a mixture of poly(L-histidine)-*b*-poly(L-lactide)-*b*-poly(ethylene glycol). *Eur. J. Pharm. Biopharm.* **2009**, *71* (2), 223−230.
(20) Lo, C. L.; et al. Mixed micelles formed from graft and diblock copolymers for application in intracellular drug delivery. *Biomaterials* **2007**, *28* (6), 1225−1235.
(21) Lo, C. L.; et al. Mixed micelle systems formed from critical micelle concentration and temperature-sensitive diblock copolymers for doxorubicin delivery. *Biomaterials* **2009**, *30* (23−24), 3961−3970.
(22) Tsai, H. C.; et al. Graft and diblock copolymer multifunctional micelles for cancer chemotherapy and imaging. *Biomaterials* **2010**, *31* (8), 2293−2301.
(23) Li, J.; et al. Synthesis and characterization of new biodegradable amphiphilic poly(ethylene oxide)-*b*-poly (*R*)-3-hydroxy butyratel-*b*-poly(ethylene oxide) triblock copolymers. *Macromolecules* **2003**, *36* (8), 2661−2667.
(24) Li, X.; et al. Dynamic and static light scattering studies on self-aggregation behavior of biodegradable amphiphilic poly(ethylene oxide)-poly (*R*)-3-hydroxybutyrate -poly(ethylene oxide) triblock copolymers in aqueous solution. *J. Phys. Chem. B* **2006**, *110* (12), 5920−5926.
(25) Rodriguez, V. B.; et al. Encapsulation and stabilization of indocyanine green within poly(styrene-alt-maleic anhydride) block-poly(styrene) micelles for near-infrared imaging. *J. Biomed. Opt.* **2008**, *13* (1), 014025.
(26) Dubochet, J.; et al. Cryo-electron microscopy of vitrified specimens. *Q. Rev. Biophys.* **1988**, *21* (2), 129−228.
(27) Holland, P. M.; Rubingh, D. N. Mixed surfactant systems—an overview. *ACS Symp. Ser.* **1992**, *501*, 2−30.
(28) Cherrick, G. R.; et al. Indocyanine green: observations on its physical properties, plasma decay, and hepatic extractions. *J. Clin. Invest.* **1959**, *39* (4), 592−600.
(29) Kirchherr, A. K.; Briel, A.; Mader, K. Stabilization of Indocyanine Green by Encapsulation within Micellar Systems. *Mol. Pharmaceutics* **2009**, *6* (2), 480−491.
(30) Altinoglu, E. I.; Adair, J. H. Near infrared imaging with nanoparticles. *WIREs Nanomed. Nanobiotechnol.* **2010**, *2* (5), 461−477.
(31) Alexandridis, P.; Hatton, T. A. Poly(ethylene oxide)-poly(propylene oxide)-poly(ethylene oxide) block-copolymer surfactants in aqueous-solutions and at interfaces—thermodynamics, structure, dynamics, and modeling. *Colloids Surf., A* **1995**, *96* (1−2), 1−46.
(32) Attwood, D.; Collett, J. H.; Tait, C. J. The micellar properties of the poly(oxyethylene) poly(oxypropylene) copolymer pluronic-F127 in water and electrolyte solution. *Int. J. Pharm.* **1985**, *26* (1−2), 25−33.
(33) Jain, S.; Bates, F. S. On the origins of morphological complexity in block copolymer surfactants. *Science* **2003**, *300* (5618), 460−464.
(34) Rajagopal, K.; et al. Curvature-Coupled Hydration of Semicrystalline Polymer Amphiphiles Yields flexible Worm Micelles but Favors Rigid Vesicles: Polycaprolactone-Based Block Copolymers. *Macromolecules* **2010**, *43* (23), 9736−9746.
(35) Massey, J. A.; et al. Self-assembly of organometallic block copolymers: The role of crystallinity of the core-forming polyferrocene block in the micellar morphologies formed by poly(ferrocenylsilane-*b*-dimethylsiloxane) in *n*-alkane solvents. *J. Am. Chem. Soc.* **2000**, *122* (47), 11577−11584.
(36) Chen, C.; et al. Preparation and characterization of biodegradable nanoparticles based on amphiphilic poly(3-hydroxybutyrate)-poly(ethylene glycol)-poly(3-hydroxybutyrate) triblock copolymer. *Eur. Polym. J.* **2006**, *42* (10), 2211−2220.
(37) Zhang, J.; et al. Micellization phenomena of amphiphilic block copolymers based on methoxy poly(ethylene glycol) and either crystalline or amorphous poly(caprolactone-*b*-lactide). *Biomacromolecules* **2006**, *7* (9), 2492−2500.
(38) Li, J.; et al. Micellization phenomena of biodegradable amphiphilic triblock copolymers consisting of poly(beta-hydroxyalkanoic acid) and poly(ethylene oxide). *Langmuir* **2005**, *21* (19), 8681−8685.
(39) Ravenelle, F.; Marchessault, R. H. Self-assembly of poly([R]-3-hydroxybutyric acid)-block-poly(ethylene glycol) diblock copolymers. *Biomacromolecules* **2003**, *4* (3), 856−858.
(40) Medintz, I. L.; et al. Self-assembled nanoscale biosensors based on quantum dot FRET donors. *Nat. Mater.* **2003**, *2* (9), 630−638.
(41) Saxena, V.; Sadoqi, M.; Shao, J. Enhanced photo-stability, thermal-stability and aqueous-stability of indocyanine green in polymeric nanoparticulate systems. *J. Photochem. Photobiol., B* **2004**, *74* (1), 29−38.
(42) Saxena, V.; Sadoqi, M.; Shao, J. Degradation kinetics of indocyanine green in aqueous solution. *J. Pharm. Sci.* **2003**, *92* (10), 2090−7.
(43) Kwon, G.; et al. Enhanced tumor accumulation and prolonged circulation times of micelle-forming poly(ethylene oxide-aspartate) block copolymer-adriamycin conjugates. *J. Controlled Release* **1994**, *29* (1−2), 17−23.
(44) Maeda, H.; et al. Tumor vascular permeability and the EPR effect in macromolecular therapeutics: a review. *J. Controlled Release* **2000**, *65* (1−2), 271−284.
(45) Torchilin, V. P. Structure and design of polymeric surfactant-based drug delivery systems. *J. Controlled Release* **2001**, *73* (2−3), 137−172.
(46) Champion, J. A.; Mitragotri, S. Shape Induced Inhibition of Phagocytosis of Polymer Particles. *Pharm. Res.* **2009**, *26* (1), 244−249.
(47) Champion, J. A.; Mitragotri, S. Role of target geometry in phagocytosis. *Proc. Natl. Acad. Sci. U.S.A.* **2006**, *103* (13), 4930−4934.
(48) Christian, D. A.; et al. Flexible Filaments for in Vivo Imaging and Delivery: Persistent Circulation of Filomicelles Opens the Dosage Window for Sustained Tumor Shrinkage. *Mol. Pharmaceutics* **2009**, *6* (5), 1343−1352.